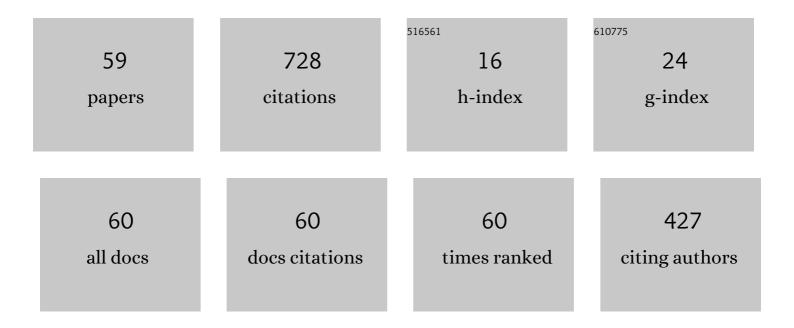
List of Publications by Year in descending order

Source: https://exaly.com/author-pdf/5839272/publications.pdf Version: 2024-02-01



SHUOYUE IIM

#	Article	IF	CITATIONS
1	Characteristics of Solar Wind Radiation Damage in Lunar Soil: PAT and TEM Study. Nanomaterials, 2022, 12, 1135.	1.9	1
2	Improving the exploration of vacancy evolution in P92 alloy under Fe ion irradiation using positron annihilation. Journal of Nuclear Materials, 2022, , 153714.	1.3	1
3	Study on the interaction between He and defects induced by He-ion irradiation in W and W5Re alloy. Fusion Engineering and Design, 2021, 162, 112118.	1.0	4
4	Study of Interaction Mechanism between Positrons and Ag Clusters in Dilute Al–Ag Alloys at Low Temperature. Materials, 2021, 14, 1451.	1.3	4
5	Correlation between Corrosion Films and Corrosion-Related Defects Formed on 316 Stainless Steel at High Temperatures in Pressurized Water. Journal of Materials Engineering and Performance, 2021, 30, 3577-3585.	1.2	9
6	Investigation of spatial relationship between helium bubbles and dislocation loops in RAFM steel. Journal of Nuclear Materials, 2021, 548, 152862.	1.3	16
7	Depth distributions of cavities in advanced ferritic/martensitic and austenitic steelsÂwith high helium preimplantation and high damage level. Materials Today Energy, 2021, 20, 100687.	2.5	11
8	The investigation of distribution on size and concentration of helium bubbles in Y-bearing ODS steel using by SAXS and GIXRD. Journal of Nuclear Materials, 2021, 554, 153083.	1.3	4
9	First-principles study of helium in austenitic Fe 6.3 at% Cr alloys: Structural, stability, energetics, and clustering with vacancies. Materials Today Communications, 2021, 29, 102837.	0.9	4
10	Characterization of oxide film in P92 ferritic-martensitic steel exposed to high temperature and pressure water. Journal of Nuclear Materials, 2020, 541, 152406.	1.3	9
11	Inhibitory effect of dislocation on helium irradiation induced damage in Fe-9†wt.Cr alloy. Fusion Engineering and Design, 2020, 161, 111978.	1.0	1
12	Stability and energetics of HenVm complexes in Fe–Cr alloys: Ab initio study. Materials Chemistry and Physics, 2020, 253, 123314.	2.0	4
13	Evolution of defects with isochronal annealing in helium-irradiated 316L studied by slow positron beam. Nuclear Instruments & Methods in Physics Research B, 2020, 467, 80-85.	0.6	5
14	Insight into structural stability and helium diffusion behavior of Fe–Cr alloys from first-principles. RSC Advances, 2020, 10, 3277-3292.	1.7	12
15	Positron Annihilation Spectroscopy Characterization of Formation of Helium/Hydrogen-Vacancy Nano-Clusters in FeCr Alloy. Acta Physica Polonica A, 2020, 137, 235-237.	0.2	4
16	Effect of interaction between H and He on micro-defects in Fe9Cr alloy investigated by slow positron beam. Journal of Nuclear Materials, 2019, 526, 151748.	1.3	12
17	Simulation for the correlation of positron annihilation rate with charge density near defects in iron. Nuclear Instruments & Methods in Physics Research B, 2019, 461, 88-92.	0.6	2
18	Influence of nanochannel structure on helium-vacancy cluster evolution and helium retention. Journal of Nuclear Materials, 2019, 527, 151822.	1.3	18

#	Article	IF	CITATIONS
19	Study on vacancy-type defects in SIMP steel induced by separate and sequential H and He ion implantation. Journal of Nuclear Materials, 2019, 520, 131-139.	1.3	21
20	Towards understanding the evolution of dislocation loops and their interaction with vacancies in Fe9Cr alloy during the irradiation swelling incubation period. Materialia, 2019, 5, 100241.	1.3	9
21	Depth synergistic effect of irradiation damage on tungsten irradiated by He-ions with various energies. Journal of Nuclear Materials, 2019, 517, 192-200.	1.3	5
22	Thermally promoted evolution of open-volume defects and Cu precipitates in the deformed FeCu alloys. Journal of Nuclear Materials, 2018, 501, 293-301.	1.3	11
23	Helium self-trapping and diffusion behaviors in deformed 316L stainless steel exposed to high flux and low energy helium plasma. Nuclear Fusion, 2018, 58, 046011.	1.6	22
24	Characterization of helium-vacancy complexes in He-ions implanted Fe9Cr by using positron annihilation spectroscopy. Journal of Nuclear Materials, 2018, 505, 69-72.	1.3	24
25	Evolution of Thermallyâ€Induced Microstructural Defects in the Feâ€9Cr Alloy. Physica Status Solidi (A) Applications and Materials Science, 2018, 215, 1700349.	0.8	6
26	Enhanced photoelectrochemical performance of TiO2 through controlled Ar+ ion irradiation: A combined experimental and theoretical study. International Journal of Hydrogen Energy, 2018, 43, 6936-6944.	3.8	11
27	Helium irradiation-induced defects in deformed 316L stainless steel. Philosophical Magazine, 2018, 98, 95-106.	0.7	5
28	Irradiation evolution of Cu precipitates in Fe1.0Cu alloy studied by positron annihilation spectroscopy. Journal of Nuclear Materials, 2018, 499, 65-70.	1.3	13
29	Effect of temperature and dose on vacancy-defect evolution in 304L stainless steel irradiated by triple ion beam. Journal of Nuclear Materials, 2018, 512, 94-99.	1.3	7
30	Thermal evolution of irradiation defects in ferritic/martensitic steel during isochronal annealing. Nuclear Instruments & Methods in Physics Research B, 2018, 436, 35-39.	0.6	7
31	Investigation of Helium Behavior in RAFM Steel by Positron Annihilation Doppler Broadening and Thermal Desorption Spectroscopy. Materials, 2018, 11, 1523.	1.3	2
32	Dissolution of M23C6 and New Phase Re-Precipitation in Fe Ion-Irradiated RAFM Steel. Metals, 2018, 8, 349.	1.0	13
33	Formation and recovery of Cu precipitates in Fe–Cu model alloys under varying heat treatment. Physica Status Solidi (A) Applications and Materials Science, 2017, 214, 1600785.	0.8	5
34	Detection of helium in irradiated Fe9Cr alloys by coincidence Doppler broadening of slow positron annihilation. Applied Physics A: Materials Science and Processing, 2017, 123, 1.	1.1	24
35	The influence of dislocation and hydrogen on thermal helium desorption behavior in Fe9Cr alloys. Journal of Nuclear Materials, 2017, 495, 244-248.	1.3	12
36	Effect of annealing on Cu precipitates in H ion irradiated Fe–0.6%Cu studied by positron annihilation. Journal of Nuclear Materials, 2016, 479, 390-393.	1.3	5

#	Article	IF	CITATIONS
37	Effect of dislocations on helium retention in deformed pure iron. Journal of Nuclear Materials, 2016, 482, 93-98.	1.3	21
38	Correlation between Cu precipitates and irradiation defects in Fe–Cu model alloys investigated by positron annihilation spectroscopy. Acta Materialia, 2016, 103, 658-664.	3.8	78
39	Helium/hydrogen synergistic effect in reduced activation ferritic/martensitic steel investigated by slow positron beam. Philosophical Magazine, 2016, 96, 253-260.	0.7	27
40	Investigation of vacancy-type defects in helium irradiated FeCrNi alloy by slow positron beam. Journal of Nuclear Materials, 2015, 458, 240-244.	1.3	42
41	Effect of annealing on V m H n complexes in hydrogen ion irradiated Fe and Fe–0.3%Cu alloys. Journal of Nuclear Materials, 2015, 459, 301-305.	1.3	16
42	The evolution of micro defects in He + irradiated FeCrNi alloy during isochronal annealing. Nuclear Instruments & Methods in Physics Research B, 2015, 356-357, 94-98.	0.6	5
43	Helium retention and thermal desorption from defects in Fe9Cr binary alloys. Journal of Nuclear Materials, 2015, 466, 522-525.	1.3	29
44	Positron beam Doppler broadening spectra and nano-hardness study on helium and hydrogen irradiated RAFM steel. Radiation Physics and Chemistry, 2015, 107, 19-22.	1.4	9
45	Effects of Ti element on the microstructural stability of 9Cr–WVTiN reduced activation martensitic steel under ion irradiation. Journal of Nuclear Materials, 2014, 455, 37-40.	1.3	4
46	Microstructural evolution of reduced-activation martensitic steel under single and sequential ion irradiations. Nuclear Instruments & Methods in Physics Research B, 2013, 307, 531-535.	0.6	2
47	Effect of annealing temperature on the ferromagnetism of Co-implanted silicon. Nuclear Instruments & Methods in Physics Research B, 2013, 307, 404-407.	0.6	1
48	Evolution of precipitate in nickel-base alloy 718 irradiated with argon ions at elevated temperature. Nuclear Instruments & Methods in Physics Research B, 2013, 307, 522-525.	0.6	10
49	Ion irradiation-induced precipitation of Cr23C6 at dislocation loops in austenitic steel. Scripta Materialia, 2013, 68, 138-141.	2.6	32
50	Enhancement of room temperature ferromagnetism in Mn-implanted Si by He implantation. Applied Physics Letters, 2012, 101, 132413.	1.5	6
51	Structural Characterization of Nickel-Base Alloy C-276 Irradiated with Ar Ions. Plasma Science and Technology, 2012, 14, 548-552.	0.7	5
52	TEM Characterization of Self-ion Irradiation Damage in Nickel-base Alloy C-276 at Elevated Temperature. Journal of Materials Science and Technology, 2012, 28, 1039-1045.	5.6	22
53	Microstructural evolution in nickel alloy C-276 after Ar-ion irradiation at elevated temperature. Materials Characterization, 2012, 72, 8-14.	1.9	18
54	Microstructural evolution of P92 ferritic/martensitic steel under Ar+ ion irradiation at elevated temperature. Materials Characterization, 2012, 68, 63-70.	1.9	21

#	Article	IF	CITATIONS
55	Microstructural evolution of P92 ferritic/martensitic steel under argon ion irradiation. Materials Characterization, 2011, 62, 136-142.	1.9	28
56	Microstructural evolution in nickel alloy C-276 after Ar+ ion irradiation. Nuclear Instruments & Methods in Physics Research B, 2011, 269, 209-215.	0.6	29
57	Neutron Diffraction and SEM Study on CaO-Al2O3-SiO2(ZnO-BaO-Na2O) Glass-Ceramics Prepared Under Different Cooling Conditions. , 2010, , .		0
58	Cu precipitates in hydrogen ion irradiated Fe–0.3%Cu alloy investigated by positron annihilation spectroscopy. , 0, , .		0
59	Energy loss correction on multiple Coulomb scattering of muons simulated by Geant4. Physica Scripta, 0, , .	1.2	0